Pharmaceutical Research, Vol. 25, No. 11, November 2008 (© 2008)
DOI: 10.1007/s11095-008-9688-y

Research Paper

Development of a Smart Nano-vehicle to Target Cerebrovascular Amyloid Deposits and Brain Parenchymal Plaques Observed in Alzheimer's Disease and Cerebral Amyloid Angiopathy

Edward K. Agyare,[1] Geoffry L. Curran,[2] Muthu Ramakrishnan,[2] Caroline C. Yu,[3] Joseph F. Poduslo,[2] and Karunya K. Kandimalla[1,2,4]

Received February 20, 2008; accepted July 14, 2008; published online August 20, 2008

Purpose. To design a smart nano-vehicle (SNV) capable of permeating the blood-brain barrier (BBB) to target cerebrovascular amyloid formed in both Alzheimer's disease (AD) and cerebrovascular amyloid angiopathy (CAA).
Methods. SNV consists of a chitosan polymeric core prepared through ionic gelation with tripolyphosphate. A polyamine modified F(ab') portion of IgG4.1, an anti-amyloid antibody, was coated as a biosensor on the SNV surface. A similar polymeric core coated with bovine serum albumin (BSA) served as a control nano-vehicle (CNV). The BBB uptake of ^{125}I-SNVs and ^{125}I-CNVs was evaluated in mice. The uptake and transcytosis of SNVs and CNVs across bovine brain microvascular endothelial cells (BBMECs) was evaluated using flow cytometry and confocal microscopy.
Results. Plasma clearance of ^{125}I-SNVs was nine times higher than that of the ^{125}I-CNVs. However, the uptake of ^{125}I-SNVs in various brain regions was about 8 to 11 times higher than that of ^{125}I-CNVs. The uptake of FITC-BSA loaded SNVs in BBMECs was twice the uptake of FITC-BSA loaded CNVs. Confocal micrographs demonstrated the uptake and transcytosis of Alexa Fluor 647 labeled SNVs, but not CNVs, across the BBMEC monolayer.
Conclusions. SNVs are capable of carrying a payload of model protein across the BBB to target cerebral amyloid.

KEY WORDS: Alzheimer's disease; blood brain barrier; brain delivery; cerebral amyloid angiopathy; chitosan nanoparticles.

INTRODUCTION

Accumulation of amyloid β-protein (Aβ) in the cerebral vasculature is a common pathological feature of Alzheimer's disease (AD) and cerebral amyloid angiopathy (CAA) (1–3). The Aβ proteins are derived from the amyloid precursor protein (APP), an integral membrane protein, through sequential proteolytic processing mediated by β-and γ-secretases (1,4). In the cerebral vasculature, Aβ proteins are deposited in the media and adventitia of small- and mid-sized arteries of the cortex and the leptomenings, which results in thickening of the basal membrane, stenosis of the vessel lumen, and fragmentation of the internal elastic lamina. These pathological changes in the cerebral vasculature may lead to brain hemorrhage, stroke, or dementia (5,6). Recent studies have suggested that cerebral microvascular amyloid may be responsible for a significant proportion of cerebral hemorrhages occurring in non-hypertensive individuals (3,7).

Currently, there is no biological marker or treatment for vascular dementia (VD) caused by CAA, and definitive diagnoses are only made upon autopsy (8). While novel diagnostic and therapeutic agents are being developed to diagnose or treat CAA, targeting them to the amyloid deposits in the vascular smooth muscle is very challenging. The foremost barrier encountered by these agents to reach vascular amyloid is the cerebrovascular endothelium, which constitutes the blood-brain barrier (BBB) with well formed paracellular tight junctions.

Because of their ability to deliver high drug payloads, polymeric nanoparticles can be promising candidates in the diagnosis and treatment of VD, if they are adeptly engineered to cross the BBB (9–11). However, selective targeting of these nanoparticles to cerebrovascular amyloid deposits remains a challenge which is addressed in this study through the development of smart nano-vehicles (SNVs). The SNV consists of a diagnostic agent coated on the surface and/or a drug entrapped in its biocompatible polymeric core, which is designed with appropriate surface characteristics and size. A biosensor, which can detect amyloid deposits, can be coated

[1] Division of Pharmaceutical Sciences, College of Pharmacy, Florida A&M University, 228 Dyson Building, Tallahassee, FL 32307, USA.
[2] Molecular Neurobiology Laboratory, Department of Neurology, Mayo Clinic College of Medicine, Rochester, MN 55905, USA.
[3] Cell Applications Inc., San Diego, CA 92121, USA.
[4] To whom correspondence should be addressed. (e-mail: Karunya.kandimalla@famu.edu)

on the surface of the polymeric core. The biosensor facilitates SNV targeting specifically to the pathological tissue ridden with amyloid deposits.

We have chosen chitosan to prepare the polymeric core, because it is biocompatible and does not cause allergic reactions. Moreover, chitosan is bioadhesive and known to improve drug absorption at cellular barriers mostly due to its high positive charge density (12). Another advantage of chitosan nanoparticles (CPCs) is that they can be prepared under exceptionally mild conditions (13), which helps ensure the integrity of delicate compounds such as peptides, proteins, DNA, and SiRNA.

The polymeric core was coated with a $F(ab')_2$ fragment of Aβ antibody (IgG4.1) modified with putrescine, referred to as $pF(ab')_2$4.1. Poduslo and associates (14) have reported that upon intravenous administration (IV) in AD transgenic mice, $pF(ab')_2$4.1 can cross the BBB, locate and bind to the cerebrovascular amyloid deposits as well as the amyloid plaques in brain parenchyma. Based on this information, we hypothesize that SNVs coated with $pF(ab')_2$4.1 can cross the BBB endothelial cells to target diagnostic and/or therapeutic agents to the amyloid vascular deposits located in the cerebral vasculature.

MATERIALS AND METHODS

Materials

Medium molecular weight chitosan (degree of deacetylation 84.5%), pentasodium tripolyphosphate (TPP) and fluorescein-isothiocyanate bovine serum albumin (FITC-BSA) were purchased from Sigma-Aldrich (St. Louis, USA). Bovine plasma fibronectin and Rat tail collagen (type 1) were purchased from Sigma-Aldrich (St. Louis, USA). The Alexa Fluor 647 (AF647) labeling kit was obtained from Invitrogen (Carlsbad, CA).

Animals

The wild type (B6/SJL) female mice at 16 weeks of age were obtained from Jackson Laboratory (Bar Harbour, ME). The animals were housed in a virus-free, light and temperature controlled barrier environment. They were provided with free access to food and water. All procedures with animals were in strict accordance with National Institutes of Health Guide for the Care and Use of Laboratory animals and were approved by the Mayo Institutional Animal Care and Use Committee.

Bovine Brain Microvascular Endothelial Cell Culture

The bovine brain microvascular endothelial (BBME) cells were obtained frozen from the Cell Applications Inc. (San Diego, CA) after the 2nd passage and were cultured in a mixture of 45% DMEM and 45% F-12 Ham nutrient mix (Gibco, Life Technology, Grand Island, IL) supplemented with 10 mM HEPES, 13 mM sodium bicarbonate, 10% donor horse serum, 100 μg/ml heparin, 100 μg/ml streptomycin, 100 μg/ml penicillin G and 2.5 μg/ml amphotericin B (Sigma-Aldrich, St. Louis, USA). The cells were plated in 75 cm^2 culture flask coated with gelatin and grown at 37°C under 95% humidity and 5% CO_2. The experiments were conducted when the cells reached about 80% confluence.

In vitro BBB Model

The filter membrane (0.4 μm) of each 12 mm Transwell® insert (Costar, Cambridge, MA) was coated with type 1 rat tail collagen and bovine fibronectin. BBMECs were then seeded on the filter membrane at a density of 70,000 to 80,000 cells/cm^2. The growth medium was added to both donor (0.5 ml) and receiver compartments (1.5 ml) and incubated at 37°C under 5% CO_2 until the monolayers were formed. A well formed monolayer was selected based on the low permeability of Lucifer yellow, a paracellular diffusion marker, and high transendothelial electrical resistance (TEER) values. The BBMEC monolayers with average TEER values below 130 Ω cm^2 were rejected.

Preparation of Chitosan Polymeric Core

Chitosan polymeric core was prepared by ionotropic gelation of chitosan with TPP according to the procedure reported by Calvo and his associates (13). The formulation components were optimized to yield the smallest size nanoparticles. For this purpose, 1% acetic acid aqueous solutions containing various chitosan concentrations: 0.1%, 0.15%, 0.2%, 0.25% and 0.3% (*w*/*v*) were prepared. The pH of each chitosan solution was adjusted to 5.5 using 1N NaOH. A 0.01% solution of TPP was also prepared in purified water. Blank nanoparticles were formed spontaneously upon addition of 3 ml of TPP solution to 6 ml of chitosan solution under constant stirring (500 rpm) at room temperature.

Characterization of CPCs

Transmission Electron Microscopy. The morphological examination of the CPCs was performed using high resolution transmission electron microscopy (TEM). The samples were stained with 1% (*w*/*v*) phosphotungstic acid after adjusting the pH of chitosan nanoparticle suspension to 7.0. The stained sample was then placed on copper grids, allowed to dry and viewed by Tecnai F-20 transmission electron microscope (Philips Co. Japan).

Laser Confocal Microscopy. An aliquot of FITC-BSA loaded CPC suspension was placed on a coverslip bottom culture dish. After settling to the bottom of the dish, the particles were imaged with LSM 510 confocal microscope (Carl Zeiss, Inc; Oberkochen, Germany) using argon/krypton laser and 100X objective.

Preparation of $pF(ab')_2$4.1 Fragments

The $pF(ab')_2$4.1 was synthesized from monoclonal IgG4.1 by a previously reported procedure (14). In brief, ficin (pH 6.5) was used to remove the Fc region from IgG4.1. The F(ab′) portion was purified and evaluated using 7.5% SDS-PAGE, and its concentration was determined using BCA protein assay (Pierce Biotechnology). The $F(ab')_2$4.1 was modified with putrescine using carbodiimide reaction to yield putrescine-$F(ab')_2$4.1 ($pF(ab')_2$4.1).

Labeling of BSA and pF(ab)$_2$4.1

The pF(ab')$_2$4.1 (500 μg) and BSA (500 μg) were labeled with ^{125}I (PerkinElmer Life and Analytical Sciences, Boston, MA) using the chloramine-T procedure as reported previously (15). Free ^{125}I was separated from the radiolabeled protein by dialysis against 0.01 M phosphate-buffered saline (PBS) at pH 7.4 (Sigma-Aldrich, St. Louis, MO). Purity of the radiolabeled proteins was determined by trichloroacetic acid (TCA) precipitation method. The radiolabeled protein was deemed acceptable, if the TCA precipitable counts were greater than 95% of the total counts. The final radioactivity associated with ^{125}I labeled pF(ab)$_2$4.1 or BSA was determined to be 10 mCi/ml.

The AF647 was conjugated to pF(ab)$_2$4.1 according to the protocol recommended by the manufacturer.

Preparation of CNVs and SNVs

The smart nano-vehicles (SNVs) or control nano-vehicles (CNVs) were formed spontaneously upon addition of 3 ml of TPP aqueous solution (1 mg/ml) to 6 ml of 1.5 mg/ml chitosan solution followed by the addition of 39 μl pF(ab')$_2$4.1 (6.28 μg/μl, pH=7.0), to form SNVs, or 500 μl of BSA (0.5 mg/ml, pH=5.5), to form CNVs, under constant stirring at room temperature. The nanoparticles formed spontaneously, were concentrated by ultracentrifugation at 10,000 rpm for 15 min. The supernatants were discarded and the CNVs and SNVs were resuspended in purified water for further characterization.

Association Efficiency of Biosensor to the Nano-vehicles

The association of BSA or pF(ab')$_2$4.1 on CNVs or SNVs, respectively, was determined using ^{125}I-labeled proteins. The nanovehicles were prepared as described above and were separated from the free protein by ultracentrifugation (30,000 rpm) at 10°C for 30 min. The activity of free ^{125}I-BSA or ^{125}I-pF(ab')$_2$4.1 was measured in the supernatant using a two-channel gamma counter, following TCA precipitation. The ^{125}I-BSA or ^{125}I-pF(ab')$_2$4.1 association efficiency (AE) with chitosan nanoparticles was calculated based on the following equation:

$$AE = \frac{Total\,protein - Free\,protein}{Total\,protein} \times 100 \qquad (1)$$

Preparation of FITC-BSA Loaded CNVs and SNVs

The FITC-BSA loaded CNVs (FITC-BSA-CNV) were formed spontaneously when 3 ml of 1 mg/ml TPP was added to 6 ml of 1.5 mg/ml chitosan solution containing 0.5 mg/ml of FITC-BSA (pH=5.5) under constant stirring. The FITC-BSA loaded SNVs (FITC-BSA-SNV) were formed by the same procedure with an exception that 39 μl of pF(ab')$_2$4.1 (6.28 μg/μl) was added to the chitosan solution after the addition of TPP. The solution was centrifuged and the FITC-BSA-CNV or SNV pellet was suspended in distilled water.

Release of BSA and pF(ab')$_2$4.1 from the Nanovehicles

In vitro release of entrapped FITC-BSA from CPCs was determined by diluting 3 ml (3.7 mg) of FITC-BSA-CPC suspension to 20 ml with PBS to maintain sink conditions. The resultant solution was transferred to a glass container with a screw-top cap and incubated at 37 °C under constant stirring (200 rpm). At appropriate time intervals (0.5, 1, 2, 4, 8, 16, 24 h), 1 ml of the sample was taken and filtered through 0.2 μm syringe filter (25 mm), which had been previously saturated with 1% solution of BSA and sucrose in PBS. The sample was replaced by 1 ml of fresh PBS pre-warmed to 37 °C. The filtrate was measured for FITC-BSA using Tecan GENios fluorescence plate reader (Tecan, San Jose, CA). The stability of BSA coating on the surface of CNVs was assessed by a similar procedure, but using FITC-BSA, because of assay limitation with unlabeled BSA. The stability of ^{125}I-BSA or ^{125}I-pF(ab')$_2$4.1 coating on ^{125}I-CNVs or ^{125}I-SNVs, respectively was also tested using a similar procedure. The ^{125}I labeled protein released from the surface of nano-vehicles was assayed using a two-channel gamma counter.

Particle Size and Zeta Potential of Nano-vehicles

The effective diameter of various nano-vehicles was determined using photon correlation spectroscopy (Particle sizer; Brookhaven Instruments, NY, US), whereas the zeta potential was determined by laser Doppler anemometry using Zeta potential Analyzer (Brookhaven Instruments, NY, US).

Blood Brain Barrier Permeability of CNVs and SNVs

The nano-vehicles for *in vivo* studies were prepared by coating ^{125}I labeled BSA (^{125}I-CNVs) or pF(ab')$_2$4.1 (^{125}I-SNVs). The femoral vein and artery of each mouse were catheterized under general anesthesia (isoflurane=1.5% and oxygen=4 l/min). The ^{125}I-SNV (125 μCi) or ^{125}I-CNVs (125 μCi) were administered intravenously in the femoral vein. Blood was sampled (20 μl) from the femoral artery of each mouse at various time intervals (0.5, 1, 3, 5, 10, 15, 30 and 40 min). The blood samples were diluted to a volume of 100 μl with normal saline, the plasma was separated by centrifugation, and analyzed for ^{125}I activity using a two-channel gamma counter (Cobra II; Amersham Biosciences Inc., Piscataway, NJ). The accumulation of ^{125}I-SNV or ^{125}I-CNVs in each brain regions was determined by perfusing the animals with normal saline at the end of the experiment. The brain of each animal was removed from the cranial cavity; dissected into various anatomical regions (cortex, caudate putamen, hippocampus, thalamus, brain stem, and cerebellum); and analyzed for ^{125}I radioactivity.

Uptake of FITC-BSA Loaded CNVs and SNVs by BBME Cells *In vitro*

BBME cells were plated at a density of 3.4×10^5 cells/cm^2 on gelatin coated six-well plates. Uptake experiments were conducted when the cells reached about 80% confluence. Before the experiment, the cells were washed three times with Hanks balanced salt solution (HBSS) pre-warmed to 37 °C and incubated at the same temperature for 30 min under 95%

humidity and 5% CO_2. The uptake study was initiated by replacing the incubate with 3 ml donor solution containing FITC-BSA-CNVs or FITC-BSA-SNV in HBSS at 30 min. After 30 min, the study was terminated by washing the endothelial cell layer three times with ice-cold PBS and then with ice-cold acidic buffer (0.2 M glycine+0.15 M NaCl; pH 3) to remove any surface bound nano-vehicles. The cells were subsequently trypsinized, suspended in ice-cold PBS, and analyzed unfixed by flow cytometry (Becton Dickinson FACS canto, San Jose, CA) equipped with 488 nm laser, dichoric mirror (502 Cp), and band-pass filter (530/30). Data from a population of viable cells, previously determined using live–dead cell assay kit (Molecular probes, Eugene, OR), was presented as histograms along with relevant statistical values such as geometric mean and coefficient variance.

Transcytosis of Nano-vehicles Across the BBMEC Monolayers

The BBMEC monolayers grown on Transwell® filters were pre-incubated for 30 min at 37 °C in HBSS buffered with 10 mM HEPES (HBSS–HEPES). Following the addition of 0.5 ml of nano-vehicle suspension (50 μg/ml) to the donor compartment and 1.5 ml fresh HBSS–HEPES to the receiver compartment, the Transwells® were incubated at 37°C upon continuous shaking at 100 rpm. After 1 h, both donor and receiver solutions were collected, and the BBMEC monolayers were washed with ice-cold acidic buffer solution (0.2 M glycine+0.15 M NaCl; pH 3) to remove any nano-vehicles adsorbed to the cell-surface. The monolayers were then fixed with 4% paraformaldehyde at 4°C for 20 min and imaged using a laser confocal microscope (Carl Zeiss MicroImaging, Inc., Thornwood, NY).

Pharmacokinetic Data Analysis

Concentrations of nanoparticles in the plasma at various time points following IV bolus administration were analyzed by noncompartmental pharmacokinetic analysis using linear trapezoidal method and uniform weighting (WinNonlin® Professional, version 5.2, Mountain view, CA). Pharmacokinetic parameters such as the plasma clearance (CL), the steady-state volume of distribution (V_d), and area under the plasma concentration curve (AUC) were also calculated using WinNonlin. The mean values of controls and treatments were compared by Student's *t*-test using GraphPad Prism.

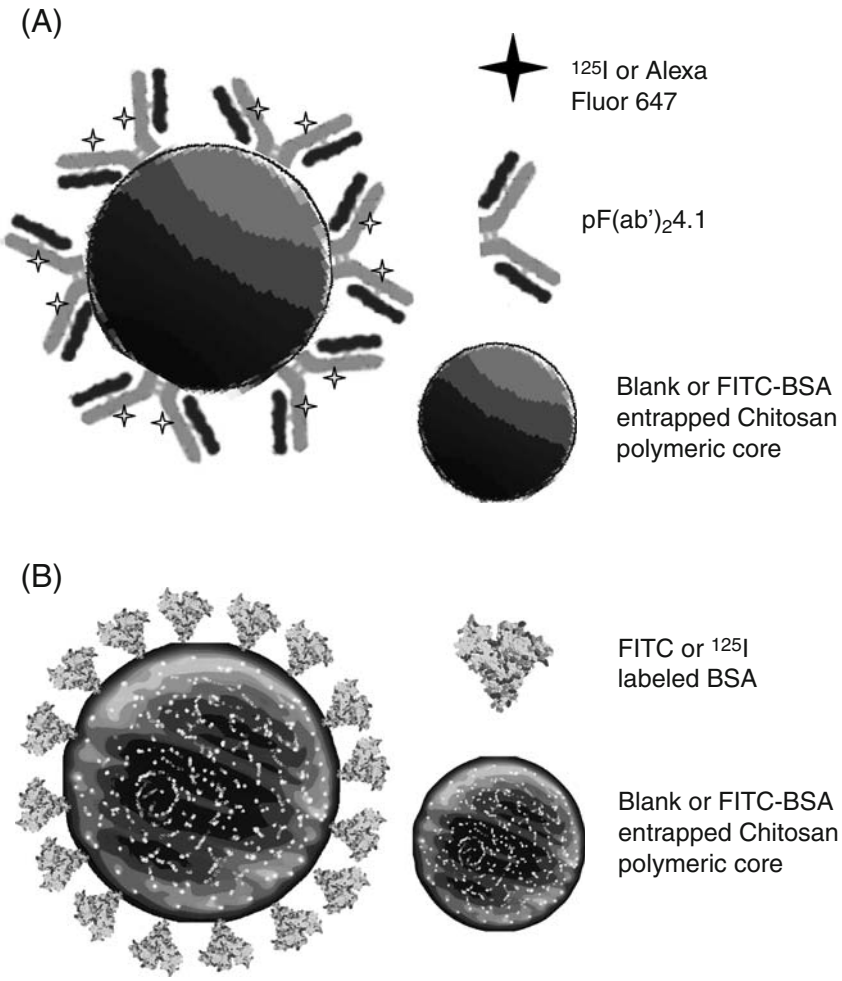

Fig. 1. A schematic of various nano-vehicles designed for the study; **A** Design of the smart nano-vehicle (SNV); **B** Design of the control nano-vehicle (CNV).

Table I. Particle Size (Average Effective Diameter) and Zeta Potential of Blank CPCs, CNVs, and SNVs Prepared at Various Chitosan Concentrations

Chitosan concentration (mg/ml)	Particle size (nm)			Zeta potential (mV)		
	Blank CPCs	CNVs	SNVs	Blank CPCs	CNVs	SNVs
3.0	744.2±28.7	684.1±136.1	555.0[a]	37.3±4.7	35.8±2.4	41.5±1.0
2.5	552.7±10.6	423.7±26.0	523.0[a]	38.8±6.9	37.2±5.5	39.5±1.5
2.0	383.9±3.5	334.6±15.2	325.1±19.2	41.0±3.4	35.9±3.3	40.0±2.6
1.5	282.1±2.3	235.7±16.3	221.6±22.5	41.1±10.8	31.7±12.2	41.6±2.6
1.0	735.2±28.1	956.1±23.3	894.0[a]	26.9±4.7	12.8±3.0	32.7±2.4

Data shown as mean ± standard deviation ($n=3$). No significant differences in particle size and zeta potential were observed among blank CPCs, CNVs and SNVs at each chitosan concentration
[a] $n=1$

Statistical Evaluation of Data

All experiments were repeated at least three times. Results are expressed as mean ± standard deviation with the exception of particle size data for SNVs where some single data points are presented. Student's *t*-test was performed to compare the means ($p<0.05$).

RESULTS

The SNVs capable of delivering a model protein (FITC-BSA) across the BBB were developed by conducting the following series of experiments: (a) formulation of a biodegradable chitosan polymeric core (CPC) with and without the entrapped FITC-BSA (Fig. 1); (b) transformation of the CPC into: SNV, ^{125}I-SNV, or AF647-SNV by coating its surface with pF(ab')$_2$4.1, ^{125}I-pF(ab')$_2$4.1, or AF647-pF(ab')$_2$4.1, respectively (Fig. 1A); (c) transformation of the CPC into FITC-BSA CNV or ^{125}I-CNV by coating the surface with FITC-BSA or ^{125}I-BSA, respectively (Fig. 1B); (d) determination of plasma pharmacokinetics and brain uptake of SNVs in comparison to CNVs; and d) determination of uptake and transcytosis of the FITC-BSA loaded SNVs and CNVs by BBME cells *in vitro*.

Formulation Optimization

Formulation of Chitosan Polymeric Core

A range of chitosan concentrations (1.0–3.0 mg/ml) were tested to arrive at the concentration that can generate the smallest polymeric core. The average effective diameter (AED) of the polymeric core decreased with decreasing chitosan concentration and yielded the smallest AED at 1.5 mg/ml (Table I). Interestingly, further decrease in chitosan concentration to 1.0 mg/ml, produced significantly larger CPCs. No significant differences in the zeta potential values were observed among CPCs formulated using various chitosan concentrations except 1.0 mg/ml, which produced significantly lower zeta potential value (Table I). Furthermore, zeta potential values were found to be dependent upon the pH of the suspension. The zeta potential values of CPCs at pH 5.0 were ~35 mV, but decreased significantly ($p<0.05$) to ~10 mV at neutral pH (Fig. 2).

FITC-BSA loaded CPCs (FITC-BSA-CPCs) also followed a similar trend and exhibited the lowest AED (208±0.41 nm) at 1.5 mg/ml chitosan concentration. The entrapment efficiency of FITC-BSA in the CPCs was found to be 69% and its release from FITC-BSA-CPCs was linear and sustained (0.133± 0.004 μg/h) for the first 18 h, but increased significantly (1.1± 0.04 μg/h) between 18–24 h (Fig. 3A). No significant initial burst release of FITC-BSA was observed.

Shape and Morphology of CPCs

The shape and morphology of CPCs were investigated by transmission electron microscopy (TEM) and laser confocal microscopy (LCM). The TEM images of various CPCs, prepared with 1.5 mg/ml chitosan solutions, are presented in Figs. 4A and B, whereas, Fig. 4C shows the confocal image of FITC-BSA entrapped CPCs prepared under similar conditions.

Formulation of SNVs and CNVs

Like CPCs, the smallest SNVs and CNVs were obtained at 1.5 mg/ml chitosan concentrations (Table I). In addition, the Zeta potential values of SNVs and CNVs were similar at various chitosan concentrations tested, except at 1.0 mg/ml where SNVs showed significantly lower zeta potential values.

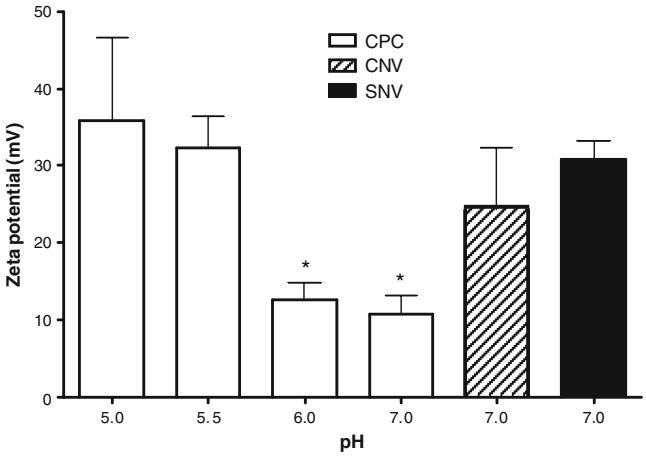

Fig. 2. Effect of pH on the zeta potential values of chitosan polymeric core (CPC), control nano-vehicle (CNV), and smart nano-vehicle (SNV). The zeta potential values of CPCs at pH 6 and 7 are significantly lower (*$p<0.05$) than the CPCs at pH 5 and 5.5 as well as CNVs or SNVs at pH 7.0. Data values expressed as mean ± SD ($n=4$).

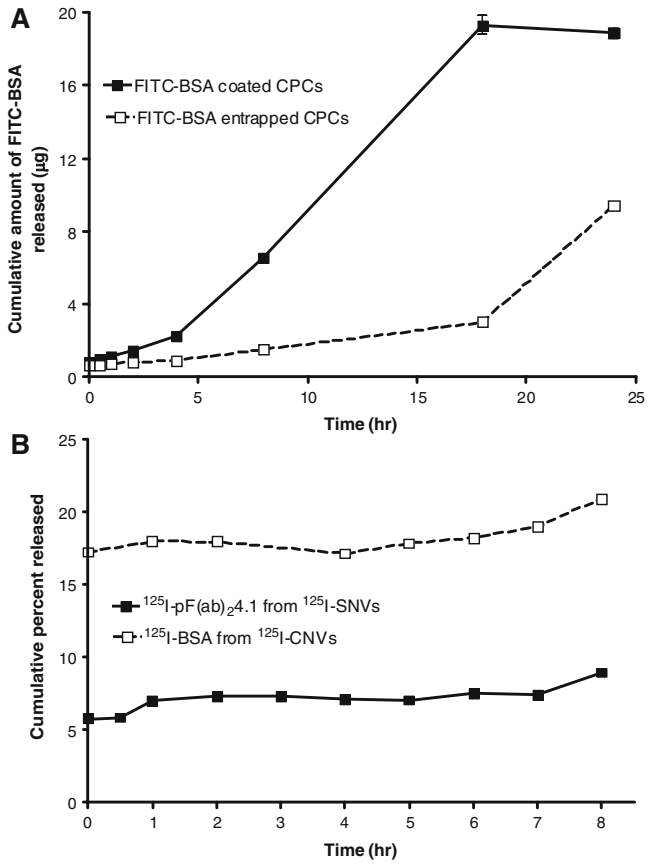

Fig. 3. **A** Cumulative amount of FITC-BSA released from FITC-BSA coated CNVs and FITC-BSA entrapped CPCs *in vitro*. **B** Release of ^{125}I-BSA and ^{125}I-pF(ab')$_2$4.1 from ^{125}I-CNVs and ^{125}I-SNVs, respectively. Data presented as mean ± SD (n=4).

The association efficiencies of pF(ab')$_2$4.1 with SNVs and BSA with CNVs were 52% and 59%, respectively. The dissociation of BSA coated on CNVs, which was determined using FITC-BSA, was biphasic with a slower rate of 0.353±0.008 µg/h for 4 h and a faster rate of 1.24±0.027 µg/h between 4 and 18 h (Fig. 3A). The dissociation of ^{125}I-pF(ab')$_2$4.1 coated on ^{125}I-SNVs was slower than that of ^{125}I-BSA (Fig. 3B). About 8% of ^{125}I-pF(ab')$_2$4.1 was released compared to 20% of ^{125}I-BSA in 8 h. These studies have demonstrated that both ^{125}I-pF(ab')$_2$4.1 and ^{125}I-BSA remain associated with the nano-vehicles for at least 5 h, which is much longer than the time frame used for the *in vitro* or *in vivo* experiments conducted in this study.

Plasma Pharmacokinetics and Brain Uptake of SNVs and CNVs

Following IV administration in mice, the ^{125}I-CNVs demonstrated a mono-exponential decline in the plasma, where as the ^{125}I-SNVs or ^{125}I-pF(ab')$_2$4.1 showed a bi-exponential decline (Fig. 5). The initial plasma concentration (C_0) of ^{125}I-SNVs was higher than that of ^{125}I-pF(ab')$_2$4.1 (Table II). While the C_0 of ^{125}I-SNVs was not significantly different from that of ^{125}I-CNVs, the plasma clearance (CL)

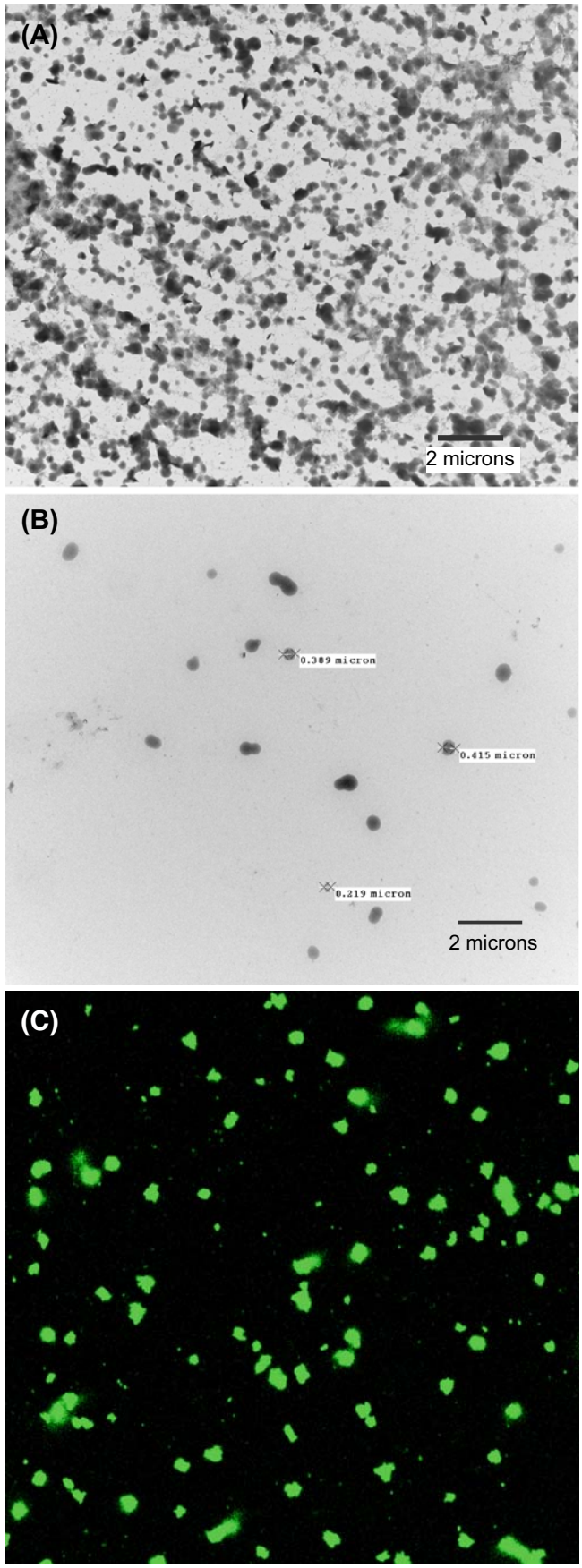

Fig. 4. Transmission electron micrographs of **A** blank CPCs (6,500×); **B** CNVs (6,500×); and **C** confocal micrograph of FITC-BSA entrapped CPCs (100×).

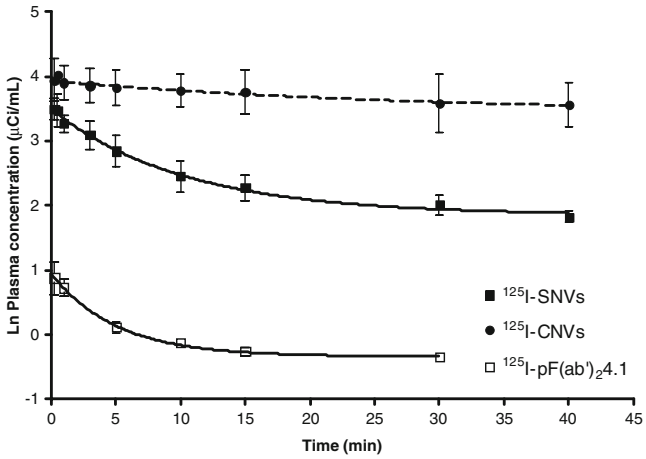

Fig. 5. Plasma pharmacokinetics of ^{125}I-CNVs, ^{125}I-SVNs and ^{125}I-pF(ab')$_2$4.1 in 16-week-old WT mice. The *dotted line* indicates a mono-exponential fit, whereas the *solid lines* represent bi-exponential fit. Data is presented as mean ± SD; (n=5).

of ^{125}I-SNVs was significantly greater than that of ^{125}I-CNVs (Table II), which is reflected by the higher accumulation of ^{125}I-SNVs in highly perfused peripheral organs such as kidney, liver, spleen, and lung (Table III). The plasma AUC of ^{125}I-CNVs was the largest, followed by that of ^{125}I-SNVs and ^{125}I-pF(ab')$_2$4.1 (Table II). The volume of distribution (V_d) of ^{125}I-pF(ab')$_2$4.1 was greater than that of ^{125}I-SNVs or ^{125}I-CNVs (Table II).

The ^{125}I-SNVs accumulated in various brain regions to a significantly greater extent than the ^{125}I-CNVs (Table IV). The brain uptake of ^{125}I-CNVs normalized with plasma AUC ranged between 5.63±1.32 and 15.52±5.32 (ml/g/min×10^{-6}) in various brain regions, whereas, the values for ^{125}I-SNVs ranged from 60.92±19.47 to 123.41±41.16 (ml/g/min×10^{-6}) and the ^{125}I-pF(ab')$_2$4.1 values ranged from 780.18±345.40 to 6137.54±2195.13 (ml/g/min×10^{-6}).

BBME Cell Uptake of SNVs and CNVs

Flow cytometry data comparing the uptake of FITC-BSA-CNVs and FITC-BSA-SNVs by the BBME cells is presented in Fig. 6. The intracellular fluorescence (A.U.=842±0.21) in trypsinized and unfixed BBMECs following the incubation with FITC-BSA-SNVs was significantly greater (Fig. 6C) than the intracellular fluorescence (A.U=464±0.87) in BBME cells incubated with FITC-BSA-CNVs (Fig. 6B). Untreated BBMECs, on the other hand, did not exhibit significant background fluorescence (Fig. 6A).

Transcytosis of Nano-vehicles Across the BBMEC Monolayer

Permeability studies were conducted to evaluate the luminal (L)–abluminal (A) transport of various nano-vehicles across the BBMEC monolayers grown on the Transwell® filter membranes. The presence of transcytosed nano-vehicles in the receiver compartment was determined by conducting a particle size analysis on the receiver solution. These studies have clearly shown that CPCs and CNVs were unable to cross the BBMEC monolayers, whereas SNVs and AF647-SNVs were able to pass through the monolayers in L–A direction (Table V). The Z-stack images of the BBMEC monolayer obtained after the transport study demonstrated the internalization of AF647-SNVs by the endothelial cells (Fig. 7, X–Y). The X–Z and Y–Z projections of the Z-stack clearly demonstrated the accumulation of AF647-SNVs towards the basement membrane of the filter (Fig. 7).

DISCUSSION

The current study is aimed at developing SNVs capable of targeting amyloid deposits in the cerebral vasculature. To reach the basal lamina of the cerebral vasculature where the amyloid deposits are located, the SNVs must be taken up by the cerebrovascular endothelial cells and be transcytosed across the BBB. We hypothesize that the transcytosis of nanoparticles at the BBB is dependent upon their size, surface morphology and ability to interact with the BBB endothelial cell surface.

Although, cellular internalization is inversely proportional to the size of the nanoparticles, the loading of diagnostic or therapeutic agents could be significantly reduced if the particle size is too small. Several published reports have indicated that particle size is also important for the retention of nanoparticles in the vascular wall (16–18). The nanoparticles around 500 nm tend to accumulate preferentially at the luminal surface, whereas 100–250 nm particles accumulate more in the adventitia of the cerebral vasculature (18,19).

Various investigators have tried to design the nanoparticles of desirable size using polymers such as polystyrene (18) and poly(butylcyanoacrylate) (PBCA) (10,20–22). However, the degradation products of these polymers such as: styrene from polystyrene (23); and acrylic acid from PBCA (24) are potentially toxic. In the current study, chitosan was

Table II. Plasma Pharmacokinetic Parameter Estimates of ^{125}I-CNVs, ^{125}I-pF(ab')$_2$4.1, and ^{125}I-SNVs Following IV Bolus Administration in WT Mice

Parameters	^{125}I-CNVs	^{125}I-pF(ab')$_2$4.1	^{125}I-SNVs	P
C_0 (μCi/ml)	56.86±18.57	2.54±0.33	38.05±10.04	^{bbb}, ns
AUC (min*μCi/ml)	1491.66±322.35	27.46±0.27	468.11±27.79	^{bbb}, ^{aaa}
CL (ml/min)	0.02±0.01	1.68±0.21	0.18±0.09	^{bbb}, ^{aaa}
V_d (ml)	1.99±0.55	115.40±8.98	4.91±1.53	^{bbb}, ^{aa}

The data is presented as mean ± S.D (n=5).
C_0 Initial concentration, *AUC* area under the curve, *CL* clearance, V_d volume of distribution, *ns* not significant
^{bbb} p<0.001 (Student's t-test; significant difference between ^{125}I-pF(ab')$_2$4.1 and ^{125}I-SNVs); ^{aa} p<0.01 (Student's t-test; significant difference between ^{125}I-CNVs and ^{125}I-SNVs); ^{aaa} p<0.001 (Student's t-test; significant difference between ^{125}I-CNVs and ^{125}I-SNVs)

Table III. Accumulation of ^{125}I-CNVs and ^{125}I-SNVs in the Peripheral Organs

Organ	^{125}I-CNVs (μCi/g)		^{125}I-SNVs (μCi/g)	
	15 min	40 min	15 min	40 min
Kidney	2.598±0.22	0.406±0.09	8.081±0.21^{aaa}	0.440±0.23^{b}
Liver	3.725±0.97	0.765±0.03	9.972±0.54^{aaa}	2.060±0.19^{bbb}
Lung	1.923±0.10	0.517±0.10	8.381±0.01^{aaa}	3.035±0.11^{bbb}
Spleen	3.272±0.56	1.351±0.18	10.987±0.18^{aaa}	3.612±0.09^{bbb}

The values are mean ± SD (n=5)
$^{aaa}p<0.001$ ((Student's t-test); ^{125}I-CNVs *versus* ^{125}I-SNVs at 15 min); $^{b}p<0.05$ ((Student's t-test); ^{125}I-CNVs *versus* ^{125}I-SNVs at 40 min); $^{bbb}p<0.001$((Student's t-test); ^{125}I-CNVs *versus* ^{125}I-SNVs at 40 min)

used to generate 250 nm sized polymeric core. Unlike the polymers mentioned above, chitosan is degraded in the body into nontoxic amino sugars (12).

Transforming the nanoparticle surface for uptake at the BBB was previously achieved by grafting a surfactant such as polysorbate 80 (21) or by conjugating antibody to a receptor expressed on the luminal surface of the BBB (25). In this study, the surface of the chitosan polymeric core (CPC) was transformed by coating with a biosensor, polyamine-modified anti-amyloid antibody fragment (pF(ab')$_2$4.1, molecular wt. ≈ 80 kDa). Poduslo and coworkers demonstrated that pF(ab')$_2$4.1 maintained excellent permeability at the BBB compared to the whole antibody (IgG4.1), the polyamine modified antibody (pIgG4.1), or the unmodified antibody fragment (F(ab')$_2$4.1), without compromising its antigen binding affinity as demonstrated by either ELISA or immunohistochemistry (14). Following IV administration in AD transgenic mice, the pF(ab')$_2$4.1 was also shown to extensively label brain parenchymal amyloid plaques as well as cerebrovascular amyloid (14). Therefore, the CPCs coated with pF(ab')$_2$4.1 on the surface are expected to permeate the BBB and locate cerebrovascular amyloid deposits; hence, they were referred to as smart nano-vehicles (SNVs). The efficacy of SNVs to cross the BBB was evaluated against CNVs, which were prepared by coating the CPCs with a nonspecific protein of similar molecular weight as pF(ab')$_2$4.1 (BSA, molecular wt. ≈ 66 kDa) (Fig. 1), but does not cross the BBB.

The adsorption and retention of pF(ab')$_2$4.1 or BSA on the surface of the CPC is very critical during the *in vitro* and *in vivo* tests conducted to evaluate differential interactions of SNVs and CNVs with endothelial cells and their ability to permeate the BBB. The extent of pF(ab')$_2$4.1 or BSA coating on the CPCs was significantly enhanced by taking advantage of the electrostatic interactions of the proteins with the CPC surface (26). For instance, BSA was added CPCs at pH 5.5 to ensure stronger interaction of positively charged amine groups present on the CPC surface with negatively charged BSA. The pF(ab')$_2$4.1 was added to CPCs at pH 6.5 when the positive charge density on the CPC surface, which can repel the cationic pF(ab')$_2$4.1, was significantly reduced.

Differential ability of ^{125}I labeled SNVs and CNVs to cross the BBB and target various brain regions was determined *in vivo* in WT mice. Substantially different plasma pharmacokinetics of ^{125}I-SNVs and ^{125}I-pF(ab')$_2$4.1 provide a convincing evidence that ^{125}I-SNV pharmacokinetics are not confounded by the plasma pharmacokinetics of free ^{125}I-pF(ab')$_2$4.1 released from the surface of the nano-vehicles. On the other hand, the plasma pharmacokinetics of ^{125}I-CNVs and ^{125}I-BSA were similar. However, according to the *in vitro* release studies, a very low amount of ^{125}I-BSA or ^{125}I-pF(ab')$_2$4.1 escapes from the surface of CNVs or SNVs, respectively in the first 5 h. The pharmacokinetic data reported in this study was obtained in a shorter time frame of 0–40 min; therefore, it is unlikely that adequate amount of free ^{125}I-BSA or ^{125}I-pF(ab')$_2$4.1 will be released from the nano-vehicles to muddle up ^{125}I-CNV or ^{125}I-SNV pharmacokinetics. Even though, the plasma residence time of ^{125}I-CNVs is greater than the ^{125}I-SNVs, the brain uptake (normalized with plasma AUC) of ^{125}I-SNVs was about eight to 14 fold greater compared to ^{125}I-CNVs. This provides a convincing evidence that the enhanced permeability of ^{125}I-SNVs

Table IV. Normalized (with Plasma AUC) Brain Uptake of ^{125}I-CNVs, ^{125}I-pF(ab')$_2$4.1 and ^{125}I-SNVs in WT Mice Following IV Bolus Injection

Brain region	Amount in the brain/AUC $_{(plasma)}$, (ml/g/min×10^{-6})			
	^{125}I-CNVs	^{125}I-SNVs	p	^{125}I-pF(ab')$_2$4.1
Cortex	15.52±5.32	123.41±41.16	^{aaa}	780.18±345.40
Caudate putamen	5.63±1.32	44.87±15.76	^{aaa}	905.42±424.62
Hippocampus	5.86±2.61	105.13±33.12	^{aaa}	1044.60±174.32
Thalamus	8.47±3.40	77.18±16.16	^{aaa}	946.14±387.35
Brain stem	12.65±6.35	60.92±19.47	^{aaa}	1370.89±418.96
Cerebellum	6.03±2.57	64.62±16.09	^{aaa}	6137.54±2195.13

Data shown as mean ± SD (n=5)
$^{aaa}p<0.001$ ((Student t-test); ^{125}I-CNVs *versus* ^{125}I-SNVs)

Table V. Transcytosis of Various Nano-vehicles Across Bovine Brain Microvascular Endothelial Cell Monolayers in Luminal-to-Abluminal Direction

	Particle size (nm)			
	CPCs	CNVs	SNVs	AF647-SNVs
Donor solution	286.4±7.8	238.4±8.2	228.6±14.9	231.2±24.7
Receiver solution	No signal	No signal	216.2±2.4	214.2±3.6

Data shown are mean ± standard deviation (n=5); no significant difference in particle size was observed among CPCs, CNVs and SNVs. No signal = no detectable levels of nano-vehicles in the receiving chamber

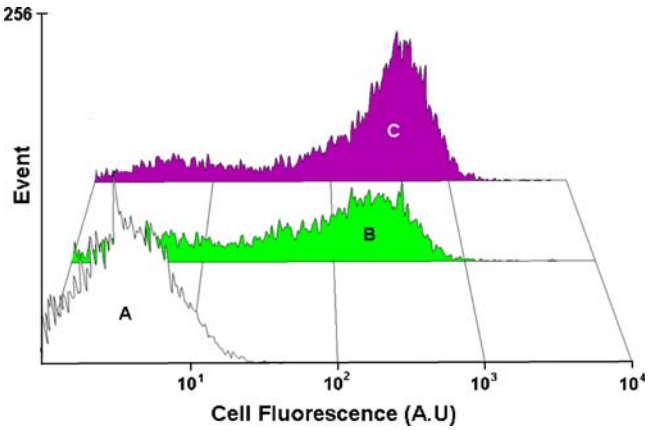

Fig. 6. Histograms of cellular fluorescence obtained from flow cytometry: **A** untreated bovine brain microvascular endothelial cells (BBMECs), **B** BBMECs treated with FITC-BSA-CNVs; and **C** BBMECs treated with FITC-BSA-SNVs. The data is presented as a geometric mean ± SD (n=5).

across the BBB is primarily a result of ^{125}I-pF(ab')$_2$4.1 coated on their surface.

The ability of SNVs to carry a model protein across the BBB was tested *in vitro* in BBME cells and also in the BBB model, which is a polarized monolayer of BBME cells grown on Transwell® inserts. FITC-BSA was used as the model protein in these experiments because: (a) it is conventionally used as a model protein to ascertain the capability of chitosan nanoparticles in transporting diagnostic or therapeutic agents across the BBB endothelial cells (27–29); and (b) to aid in the detection of SNVs and CNVs in the endothelial cells by flow cytometry or by laser confocal microscopy. The FITC-BSA loaded in these vehicles exhibited a constant release for about 18 h. This sustained release of FITC-BSA may be attributed to the stronger electrostatic interaction between the FITC-BSA and chitosan as well as the high degree of compactness of the nanoparticles which requires more time for swelling of the polymer matrix (26). The uptake of FITC-BSA-SNVs by BBMECs, determined by flow cytometry, was significantly higher than that of the FITC-BSA-CNVs. In addition, the studies conducted to evaluate the permeability of various

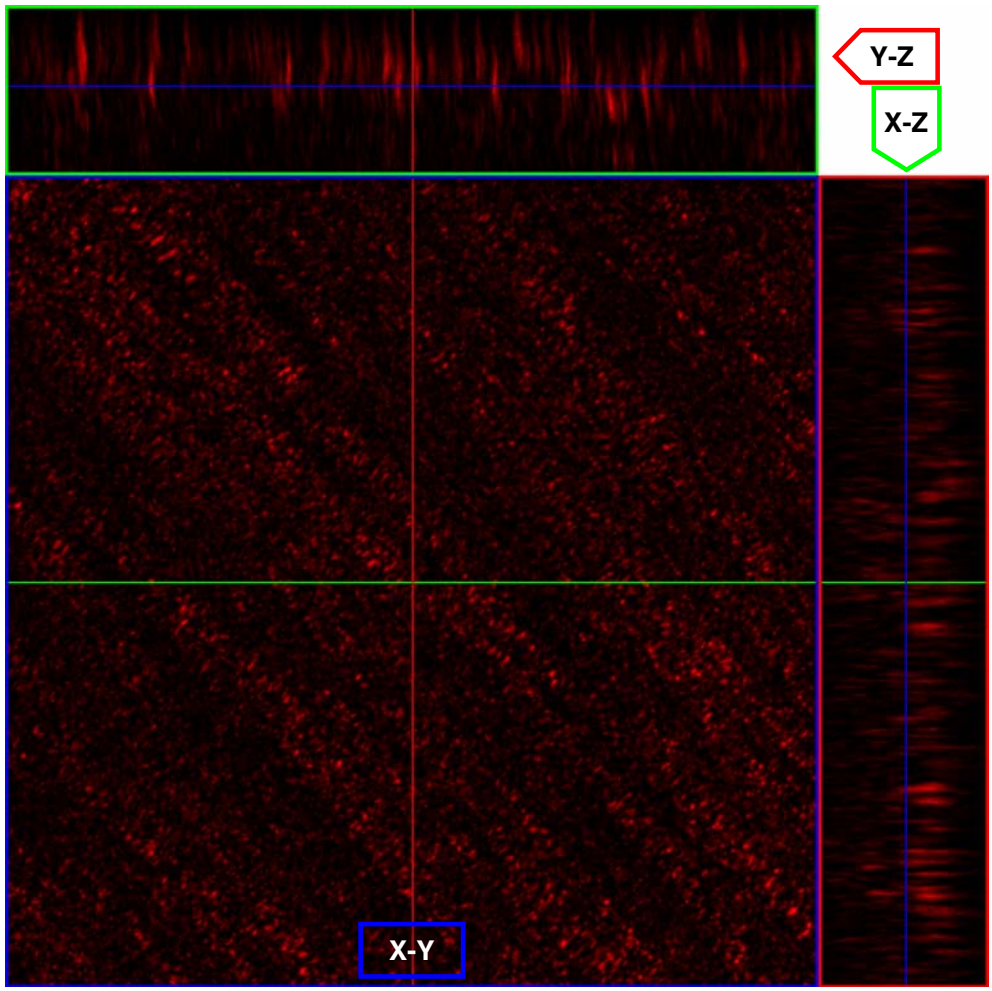

Fig. 7. Localization of SNVs labeled with Alexa Fluor 647 (AF647-SNV) in bovine brain microvascular endothelial cell (BBMEC) monolayer. Images were taken as z-stack using a 40× objective coupled with 3× digital zoom. **A** Z-stack presented in x–y plane clearly demonstrates cellular uptake of AF647-SNVs. Projection in both the x–z and y–z orthogonal planes confirms the transcytosis of AF647-SNVs across the BBMEC monolayer.

nano-vehicles across the BBB model *in vitro*, clearly demonstrated the uptake and transcytosis of SNVs but not CNVs or CPCs. These results confirmed the *in vivo* observations that pF(ab')$_2$4.1 greatly enhances the transcytosis of SNVs across the BBB.

CONCLUSION

Our studies demonstrated that the formulation of chitosan nanoparticles into SNVs increased their uptake at the BBB. Upon IV bolus injection in WT mouse, the SNVs accumulated in various brain regions to a significantly greater extent than the CNVs. *In vitro* uptake of FITC-BSA-SNVs by BBMECs was higher than the FITC-BSA entrapped CNVs. In addition, permeability studies conducted on the polarized BBMEC monolayer demonstrated the transcytosis of SNVs, but not CNVs. Together, these studies indicate that pF (ab')$_2$4.1 is responsible for enhancing the uptake and transcytosis of SNVs at the BBB endothelial cells. The knowledge gained from this study will be useful in the development of chitosan nanoparticles capable of delivering diagnostic or therapeutic agents across the BBB to target amyloid deposits in the cerebral vasculature of AD transgenic mice.

ACKNOWLEDGMENTS

This work was supported by grants from NIH/NIGMS/MBRS 3S06GM008111-35S1—(Minority Biomedical Research Support); NIH/NCRR/RCMI G12RR03020—(Research centers in Minority Institutions) faculty development grant in drug delivery; the Neuroscience Cores for MR Studies of the Brain from NINDS (NS057091); NIH R01 AG22034; and the Minnesota Partnership for Biotechnology and Medical Genomics.

REFERENCES

1. D. J. Selkoe. Alzheimer's disease results from the cerebral accumulation and cytotoxicity of amyloid beta-protein. *J. Alzheimers Dis.* **3**:75–80 (2001).
2. K. A. Jellinger. Alzheimer disease and cerebrovascular pathology: an update. *J. Neural. Transm.* **109**:813–836 (2002). doi:10.1007/s007020200068.
3. H. V. Vintersand, and E. S. Farag. Amyloidosis of cerebral arteries. *Adv. Neurol.* **92**:105–112 (2003).
4. D. J. Selkoe. Alzheimer's disease: genes, proteins, and therapy. *Physiol. Rev.* **81**:741–766 (2001).
5. E. Levy, M. Haltia, I. Fernandez-Madrid, O. Koivunen, J. Ghiso, F. Prelli, and B. Frangione. Mutation in gelsolin gene in Finnish hereditary amyloidosis. *J. Exp. Med.* **172**:1865–1867 (1990). doi:10.1084/jem.172.6.1865.
6. C. Van Broeckhoven, J. Haan, E. Bakker, J. A. Hardy, W. Van Hul, A. Wehnert, M. Vegter-Van der Vlis, and R. A. Roos. Amyloid beta protein precursor gene and hereditary cerebral hemorrhage with amyloidosis (Dutch). *Science.* **248**:1120–1122 (1990). doi:10.1126/science.1971458.
7. H. M. Wisniewski, A. W. Vorbrodt, and J. Wegiel. Amyloid angiopathy and blood-brain barrier changes in Alzheimer's disease. *Ann. N. Y. Acad. Sci.* **826**:161–172 (1997). doi:10.1111/j.1749-6632.1997.tb48468.x.
8. R. S. Turner. Biomarkers of Alzheimer's disease and mild cognitive impairment: are we there yet? *Exp. Neurol.* **183**:7–10 (2003). doi:10.1016/S0014-4886(03)00203-6.
9. C. Roney, P. Kulkarni, V. Arora, P. Antich, F. Bonte, A. Wu, N. N. Mallikarjuana, S. Manohar, H. F. Liang, A. R. Kulkarni, H. W. Sung, M. Sairam, and T. M. Aminabhavi. Targeted nanoparticles for drug delivery through the blood-brain barrier for Alzheimer's disease. *J. Control. Release.* **108**:193–214 (2005). doi:10.1016/j.jconrel.2005.07.024.
10. J. Kreuter. Nanoparticulate systems for brain delivery of drugs. *Adv. Drug. Deliv. Rev.* **47**:65–81 (2001). doi:10.1016/S0169-409X(00)00122-8.
11. J. Kreuter. Application of nanoparticles for the delivery of drugs to the brain. *Int. Congr. Ser. Drug Trans.(ers) Dis. Brain.* **1277**:85–94 (2005).
12. Y. Aktas, K. Andrieux, M. J. Alonso, P. Calvo, R. N. Gursoy, P. Couvreur, and Y. Capan. Preparation and *in vitro* evaluation of chitosan nanoparticles containing a caspase inhibitor. *Int. J. Pharm.* **298**:378–383 (2005). doi:10.1016/j.ijpharm.2005.03.027.
13. P. Calvo, C. Remunan-Lopez, J. L. Vila-Jato, and M. J. Alonso. Chitosan and chitosan/ethylene oxide–propylene oxide block copolymer nanoparticles as novel carriers for proteins and vaccines. *Pharm. Res.* **14**:1431–1436 (1997). doi:10.1023/A:1012128907225.
14. J. F. Poduslo, M. Ramakrishnan, S. S. Holasek, M. Ramirez-Alvarado, K. K. Kandimalla, E. J. Gilles, G. L. Curran, and T. M. Wengenack. *In vivo* targeting of antibody fragments to the nervous system for Alzheimer's disease immunotherapy and molecular imaging of amyloid plaques. *J. Neurochem.* **102**:420–433 (2007). doi:10.1111/j.1471-4159.2007.04591.x.
15. J. F. Poduslo, S. L. Whelan, G. L. Curran, and T. M. Wengenack. Therapeutic benefit of polyamine-modified catalase as a scavenger of hydrogen peroxide and nitric oxide in familial amyotrophic lateral sclerosis transgenics. *Ann. Neurol.* **48**:943–947 (2000). doi:10.1002/1531-8249(200012)48:6<943::AID-ANA18>3.0.CO;2-1.
16. J. J. Rome, V. Shayani, M. Y. Flugelman, K. D. Newman, A. Farb, R. Virmani, and D. A. Dichek. Anatomic barriers influence the distribution of *in vivo* gene transfer into the arterial wall. Modeling with microscopic tracer particles and verification with a recombinant adenoviral vector. *Arterioscler. Thromb.* **14**:148–161 (1994).
17. C. Song, V. Labhasetwar, X. Cui, T. Underwood, and R. J. Levy. Arterial uptake of biodegradable nanoparticles for intravascular local drug delivery: results with an acute dog model. *J. Control. Release.* **54**:201–211 (1998). doi:10.1016/S0168-3659(98)00016-9.
18. U. Westedt, L. Barbu-Tudoran, A. K. Schaper, M. Kalinowski, H. Alfke, and T. Kissel. Deposition of nanoparticles in the arterial vessel by porous balloon catheters: localization by confocal laser scanning microscopy and transmission electron microscopy. *AAPS Pharm. Sci.* **4**:E41 (2002). doi:10.1208/ps040441.
19. L. A. Guzman, V. Labhasetwar, C. Song, Y. Jang, A. M. Lincoff, R. Levy, and E. J. Topol. Local intraluminal infusion of biodegradable polymeric nanoparticles. A novel approach for prolonged drug delivery after balloon angioplasty. *Circulation.* **94**:1441–1448 (1996).
20. J. Kreuter. Drug targeting with nanoparticles. *Eur. J. Drug. Metab. Pharmacokinet.* **19**:253–256 (1994).
21. R. N. Alyautdin, V. E. Petrov, K. Langer, A. Berthold, D. A. Kharkevich, and J. Kreuter. Delivery of loperamide across the blood-brain barrier with polysorbate 80-coated polybutylcyanoacrylate nanoparticles. *Pharm. Res.* **14**:325–328 (1997). doi:10.1023/A:1012098005098.
22. B. Wilson, M. K. Samanta, K. Santhi, K. P. Kumar, N. Paramakrishnan, and B. Suresh. Poly(n-butylcyanoacrylate) nanoparticles coated with polysorbate 80 for the targeted delivery of rivastigmine into the brain to treat Alzheimer's disease. *Brain. Res.* **1200**:159–168 (2008). doi:10.1016/j.brainres.2008.01.039.
23. D. Jégaden, D. Amann, J. F. Simon, M. Habault, B. Legoux, and P. Galopin. Study of the neurobehavioural toxicity of styrene at low levels of exposure. *Int. Arch. of Occup. Environ. Health.* **64**:527–531 (1993). doi:10.1007/BF00381103.
24. J. Kreuter, P. Ramge, V. Petrov, S. Hamm, S. E. Gelperina, B. Engelhardt, R. Alyautdin, H. von Briesen, and D. J. Begley. Direct Evidence That Polysorbate-80-Coated Poly(Butylcyanoacrylate) Nanoparticles Deliver Drugs to the CNS via Specific Mechanisms Requiring Prior Binding of Drug to the Nanoparticles. *Pharm. Res.* **20**:409–416 (2003). doi:10.1023/A:1022604120952.
25. Y. Aktas, M. Yemisci, K. Andrieux, R. N. Gursoy, M. J. Alonso, E. Fernandez-Megia, R. Novoa-Carballal, E. Quinoa, R. Riguera, M. F. Sargon, H. H. Celik, A. S. Demir, A. A. Hincal, T. Dalkara, Y. Capan, and P. Couvreur. Development and brain

delivery of chitosan-PEG nanoparticles functionalized with the monoclonal antibody OX26. *Bioconjug. Chem.* **16**:1503–1511 (2005). doi:10.1021/bc050217o.
26. Q. Gan, and T. Wang. Chitosan nanoparticle as protein delivery carrier—systematic examination of fabrication conditions for efficient loading and release. *Colloids. Surf. B. Biointerfaces*. **59**:24–34 (2007). doi:10.1016/j.colsurfb.2007.04.009.
27. W. Lu, Y. Z. Tan, K. L. Hu, and X. G. Jiang. Cationic albumin conjugated pegylated nanoparticle with its transcytosis ability and little toxicity against blood-brain barrier. *Int. J. Pharm.* **295**:247–260 (2005). doi:10.1016/j.ijpharm.2005.01.043.
28. W. Lu, Y. Zhang, Y. Z. Tan, K. L. Hu, X. G. Jiang, and S. K. Fu. Cationic albumin-conjugated pegylated nanoparticles as novel drug carrier for brain delivery. *J. Control. Release.* **107**:428–448 (2005). doi:10.1016/j.jconrel.2005.03.027.
29. Y. Xu, and Y. Du. Effect of molecular structure of chitosan on protein delivery properties of chitosan nanoparticles. *Int J Pharm*. **250**:215–226 (2003). doi:10.1016/S0378-5173(02)00548-3.